

# Optically induced Kondo effect in semiconductor quantum wells

I. V. Iorsh<sup>1,2</sup> and O. V. Kibis<sup>2\*</sup>

<sup>1</sup>*Department of Physics and Engineering, ITMO University, Saint-Petersburg, 197101, Russia and*

<sup>2</sup>*Department of Applied and Theoretical Physics, Novosibirsk State Technical University, Karl Marx Avenue 20, Novosibirsk 630073, Russia*

It is demonstrated theoretically that the circularly polarized irradiation of two-dimensional electron systems can induce the localized electron states which antiferromagnetically interact with conduction electrons, resulting in the Kondo effect. Conditions of experimental observation of the effect are discussed for semiconductor quantum wells.

## I. INTRODUCTION

In 1964, Jun Kondo in his pioneering article<sup>1</sup> suggested the physical mechanism responsible for the minimum of temperature dependence of the resistivity of noble divalent metals, which had remained a mystery for more than three decades<sup>2</sup>. Within the developed theory, he showed that the antiferromagnetic interaction between the spins of conduction electrons and electrons localized on magnetic impurities leads to the  $\log(T)$  corrections to the relaxation time of conduction electrons (the Kondo effect). The subsequent studies on the subject<sup>3-5</sup> demonstrated that physics of the Kondo effect is universal to describe the transformation of the ground state of various many-body systems in the broad range of energies. Particularly, the transformation is characterized by the single energy scale  $T_K$  (the Kondo temperature) and can be effectively treated by the powerful methods of the renormalization group theory. Therefore, the Kondo problem is currently considered as an effective testing ground to solve many challenging many-body problems, including heavy-fermion materials, high-temperature superconductors, etc<sup>6-9</sup>.

The Kondo temperature is defined by the Coulomb repulsion of the impurity atoms, hybridization of the conduction and impurity electrons, and other condensed-matter parameters which are fixed in bulk materials but can be effectively tuned in nanostructures. Since the first observation of the tunable Kondo effect in such nanostructures as quantum dots<sup>11</sup>, it attracts the enormous attention of research community<sup>12-15</sup>. While the tuning of Kondo temperature in nanostructures is usually achieved by stationary fields (produced, e.g., by the gate voltage<sup>13</sup>), it should be noted that all physical properties of them can be effectively controlled also by optical methods. Particularly, it has been demonstrated that the resonant laser driving of the impurity spins (such as quantum dot spins or single atom spins in the optical lattices) allows for the control over the onset and destruction of the Kondo resonance<sup>16-20</sup>. An alternative optical way of controlling the Kondo effect could be based on the modification of electronic properties by an off-resonant high-frequency electromagnetic field (the Floquet engineering<sup>21,22</sup>), which became the established research area of modern physics and resulted in many fundamental effects in various nanostructures<sup>23-38</sup>. Since the frequency

of the off-resonant field lies far from characteristic resonant frequencies of the electron system, the field cannot be absorbed and only “dresses” electrons (dressing field), changing their physical characteristics. Particularly, it was demonstrated recently that a high-frequency circularly polarized dressing field crucially modifies the interaction of two-dimensional (2D) electron systems with repulsive scatterers, inducing the attractive area in the core of a repulsive potential<sup>39</sup>. As a consequence, the light-induced electron states localized at repulsive scatterers appear<sup>40,41</sup>. Since such localized electron states are immersed into the continuum of conduction electrons and interact with them antiferromagnetically, the Kondo effect can exist. The present article is dedicated to theoretical analysis of this optically induced effect for 2D electron gas in semiconductor quantum wells (QWs).

The article is organized as follows. In the second section, the model of Kondo effect based on the dressing field approach is developed. The third section is dedicated to the analysis of the Kondo resonance and the Kondo temperature in QWs. The last two sections contain conclusion and acknowledgements.

## II. MODEL

For definiteness, let us consider a semiconductor QW of the area  $S$  in the plane  $x, y$ , which is filled by 2D gas of conduction electrons with the effective mass  $m_e$  and irradiated by a circularly polarized electromagnetic wave incident normally to the  $x, y$  plane. Then the behavior of a conduction electron near a scatterer with the repulsive potential  $U(\mathbf{r})$  is described by the time-dependent Hamiltonian  $\hat{\mathcal{H}}_e(t) = (\hat{\mathbf{p}} - e\mathbf{A}(t)/c)^2/2m_e + U(\mathbf{r})$ , where  $\hat{\mathbf{p}}$  is the plane momentum operator of conduction electron,  $\mathbf{r} = (x, y)$  is the plane radius vector of the electron,

$$\mathbf{A}(t) = (A_x, A_y) = [cE_0/\omega_0](\sin \omega_0 t, \cos \omega_0 t) \quad (1)$$

is the vector potential of the wave,  $E_0$  is the electric field amplitude of the wave, and  $\omega_0$  is the wave frequency. If the field frequency  $\omega_0$  is high enough and lies far from characteristic resonant frequencies of the QW, this time-dependent Hamiltonian can be reduced to the effective stationary Hamiltonian,  $\hat{\mathcal{H}}_0 = \hat{\mathbf{p}}^2/2m_e + U_0(\mathbf{r})$ , where

$$U_0(\mathbf{r}) = \frac{1}{2\pi} \int_{-\pi}^{\pi} U(\mathbf{r} - \mathbf{r}_0(t)) d(\omega_0 t) \quad (2)$$

is the repulsive potential modified by the incident field (dressed potential),  $\mathbf{r}_0(t) = (-r_0 \cos \omega_0 t, r_0 \sin \omega_0 t)$  is the radius-vector describing the classical circular trajectory of a free electron in the circularly polarized field (1), and  $r_0 = |e|E_0/m_e\omega_0^2$  is the radius of the trajectory<sup>39,40</sup>. In the case of the short-range scatterers conventionally modelled by the repulsive delta potential,

$$U(\mathbf{r}) = u_0\delta(\mathbf{r}), \quad (3)$$

the corresponding dressed potential (4) reads<sup>40</sup>

$$U_0(\mathbf{r}) = \frac{u_0 \delta(r - r_0)}{2\pi r_0}. \quad (4)$$

Thus, the circularly polarized dressing field (1) turns the repulsive delta potential (3) into the delta potential barrier of ring shape (4), which defines dynamics of an electron near the scatterer. As a consequence, the bound electron states which are localized inside the area fenced by the ring-shape barrier ( $0 < r < r_0$ ) appear. Certainly, such bound electron states are quasi-stationary since they can decay via the tunnel transition through the potential barrier (4) into the continuum of conduction electrons. As a consequence, the energy broadening of the localized states appears. In the following, we will restrict the analysis by the ground localized state with the energy  $\varepsilon_0$ , the energy broadening  $\Gamma_0$  and the wave function  $\psi_0(r)$  (see Fig. 1). Assuming the repulsive delta potential to be strong enough ( $\alpha = 2\hbar^2/m_e u_0 \ll 1$ ), the solution of the Schrödinger problem with the stationary potential (4) can be written approximately as<sup>40</sup>

$$\begin{aligned} \varepsilon_0 &= \frac{\hbar^2 \xi_0^2}{2m_e r_0^2}, \quad \Gamma_0 = \frac{2\varepsilon_0 \alpha^2}{N_0^3(\xi_0) J_1(\xi_0)}, \\ \psi_0(r) &= \frac{J_0(\xi_0 r / r_0)}{\sqrt{\pi r_0} J_1(\xi_0)} \theta(r_0 - r), \end{aligned} \quad (5)$$

where  $J_m(\xi)$  and  $N_m(\xi)$  are the Bessel functions of the first and second kind, respectively,  $\xi_0$  is the first zero of the Bessel function  $J_0(\xi)$ , and  $\theta(r)$  is the Heaviside function. It follows from the theory of the dressed potential approach<sup>39</sup> that the discussed model based on the dressed potential (4) is applicable if the dressing field frequency,  $\omega_0$ , much exceeds the characteristic frequency of the bound electron state,  $\varepsilon_0/\hbar$ .

Assuming the condition  $\hbar\omega_0 \gg \varepsilon_0$  to be satisfied, interaction between the localized electron state (5) and the conduction electrons can be described by the Hamiltonian

$$\begin{aligned} \hat{\mathcal{H}} &= \sum_{\mathbf{k}, \sigma} (\varepsilon_{\mathbf{k}} - \varepsilon_F) \hat{c}_{\mathbf{k}\sigma}^\dagger \hat{c}_{\mathbf{k}\sigma} + \sum_{\sigma} (\varepsilon_0 - \varepsilon_F) \hat{d}_{\sigma}^\dagger \hat{d}_{\sigma} \\ &+ U_C \hat{d}_{\uparrow}^\dagger \hat{d}_{\uparrow} \hat{d}_{\downarrow}^\dagger \hat{d}_{\downarrow} + \sum_{\mathbf{k}, \sigma} T_{\mathbf{k}} \left[ \hat{c}_{\mathbf{k}, \sigma}^\dagger \hat{d}_{\sigma} + \text{H.c.} \right], \end{aligned} \quad (6)$$

where  $\varepsilon_{\mathbf{k}} = \hbar^2 k^2 / 2m_e$  is the energy spectrum of conduction electrons,  $\mathbf{k}$  is the electron wave vector,  $\varepsilon_F$  is the Fermi energy of conduction electrons,  $\sigma = \uparrow, \downarrow$  is the spin

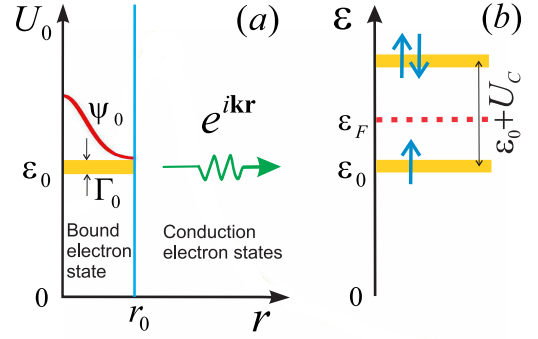


FIG. 1: Sketch of the system under consideration: (a) the optically induced potential (4) depicted by the vertical blue line, which confines the bound electron state (5) marked by the horizontal yellow strip and separates it from the states of conduction electrons with the wave vectors  $\mathbf{k}$  marked by the wave arrow; (b) the energy structure of singly-occupied ( $\uparrow$ ) and doubly occupied ( $\uparrow\downarrow$ ) electron states (5) near the Fermi energy  $\varepsilon_F$ .

quantum number,  $\hat{c}_{\mathbf{k}, \sigma}^\dagger$  ( $\hat{c}_{\mathbf{k}, \sigma}$ ) are the production (annihilation) operators for conduction electron states,  $\hat{d}_{\sigma}^\dagger$  ( $\hat{d}_{\sigma}$ ) are the production (annihilation) operators for the light-induced localized electron states (5),

$$U_C = e^2 \int_S d^2 \mathbf{r} \int_S d^2 \mathbf{r}' \frac{|\psi_0(r)|^2 |\psi_0(r')|^2}{|\mathbf{r} - \mathbf{r}'|} = \frac{\gamma e^2}{\varepsilon r_0}, \quad (7)$$

is the Coulomb interaction energy of two electrons with opposite spins  $\sigma = \uparrow, \downarrow$  in the state (5),  $\varepsilon$  is the permittivity of QW,  $\gamma \approx 0.8$  is the numerical constant, and  $T_{\mathbf{k}}$  is the tunneling matrix element connecting the localized electron state (5) and the conduction electron state with the wave vector  $\mathbf{k}$ . Physically, the first term of the Hamiltonian (6) describes the energy of conduction electrons, the second term describes the energy of the localized electron in the state (5), the third term describes the Coulomb energy shift of the double occupied state (5), and the fourth term describes the tunnel interaction between the conduction electrons and the localized electrons. Assuming the tunneling to be weak enough, one can replace the matrix element  $T_{\mathbf{k}}$  with its resonant value,  $|T_{\mathbf{k}}|^2 = \Gamma_0 / \pi N_{\varepsilon}$ , corresponding to the energy  $\varepsilon_{\mathbf{k}} = \varepsilon_0$ , where  $N_{\varepsilon} = S m_e / \pi \hbar^2$  is the density of conduction electron states (see, e.g., Appendix B in Ref. 40). If the localized and delocalized (conduction) electron states are decoupled from each other ( $T_{\mathbf{k}} = 0$ ), the localized eigenstates of the Hamiltonian (6) correspond to the singly occupied state (5) with the eigenenergy  $\varepsilon_0 - \varepsilon_F$  and the doubly occupied state (5) with the eigenenergy  $2(\varepsilon_0 - \varepsilon_F) + U_C$ , which are marked schematically in Fig. 1b by the symbols  $\uparrow$  and  $\uparrow\downarrow$ , correspondingly. For completeness, it should be noted that the empty state (5) is also the eigenstate of the considered Hamiltonian with the zero eigenenergy corresponding to the Fermi level. Since the Kondo effect originates due to the emer-

gence of magnetic moment (spin) of a localized electron, it appears only if the singly occupied state is filled by an electron but the doubly occupied state is empty. Assuming the temperature to be zero, this corresponds to the case of  $\varepsilon_0 - \varepsilon_F < 0$  and  $U_C > \varepsilon_F - \varepsilon_0$ . Taking into account that the characteristic energies of the considered problem,  $U_C$  and  $\varepsilon_0$ , depend differently on the irradiation amplitude  $E_0$  and frequency  $\omega_0$ , the optically induced Kondo effect can exist only in the range of these irradiation parameters defined by the inequality

$$\sqrt{\frac{\hbar^2 \xi_0^2}{2m_e \varepsilon_F}} < r_0 < \frac{\gamma e^2}{2\epsilon \varepsilon_F} + \sqrt{\frac{\hbar^2 \xi_0^2}{2m_e \varepsilon_F} + \left(\frac{\gamma e^2}{2\epsilon \varepsilon_F}\right)^2}. \quad (8)$$

Mathematically, the Hamiltonian (6) is identical to the famous Anderson Hamiltonian describing the microscopic mechanism for the magnetic moment formation in metals<sup>42</sup>. Therefore, one can apply the known Schrieffer-Wolff (SW) unitary transformation<sup>43</sup> to turn the Hamiltonian (6) into the Hamiltonian of the Kondo problem<sup>5</sup>. Assuming the condition (8) to be satisfied, we arrive at the Kondo Hamiltonian

$$\hat{H}_K = \sum_{\mathbf{k}\sigma} (\varepsilon_{\mathbf{k}} - \varepsilon_F) \hat{c}_{\mathbf{k}\sigma}^\dagger \hat{c}_{\mathbf{k}\sigma} + J \hat{\boldsymbol{\sigma}}(0) \cdot \mathbf{S}_0 - \frac{V}{2} \hat{\psi}_\sigma^\dagger(0) \hat{\psi}_\sigma(0), \quad (9)$$

where  $\hat{\psi}_\sigma(0) = \sum_{\mathbf{k}} \hat{c}_{\mathbf{k}\sigma}$  is the  $\hat{\psi}(\mathbf{r})$  operator of conduction electrons at the repulsive delta potential ( $\mathbf{r} = 0$ ),  $\hat{\boldsymbol{\sigma}}(0) = \hat{\psi}^\dagger(0) \hat{\boldsymbol{\sigma}} \hat{\psi}(0)$  is the spin density of conduction electrons at  $\mathbf{r} = 0$ ,  $\mathbf{S}_0 = \hat{d}^\dagger (\hat{\boldsymbol{\sigma}}/2) \hat{d}$  is the spin density of an electron in the localized state (5),  $\hat{\boldsymbol{\sigma}} = (\sigma_x, \sigma_y, \sigma_z)$  is the spin vector matrix, and the coupling coefficients  $J$  and  $V$  read

$$J = \frac{\Gamma_0}{\pi N_\varepsilon} \left[ \frac{1}{\varepsilon_0 - \varepsilon_F + U_C} + \frac{1}{\varepsilon_F - \varepsilon_0} \right], \quad (10)$$

$$V = -\frac{\Gamma_0}{2\pi N_\varepsilon} \left[ \frac{1}{\varepsilon_0 - \varepsilon_F + U_C} - \frac{1}{\varepsilon_F - \varepsilon_0} \right]. \quad (11)$$

It should be noted that the denominators in Eqs. (10)–(11) are the energy detunings between the singly occupied and empty states,  $\varepsilon_F - \varepsilon_0$ , and the singly and doubly occupied states,  $\varepsilon_0 - \varepsilon_F + U_C$ . Since excitation of the empty (doubly occupied) state creates an electron (hole) in the Fermi sea, we will label the corresponding detunings as  $D_e = \varepsilon_F - \varepsilon_0$  and  $D_h = \varepsilon_0 - \varepsilon_F + U_C$ .

It should be stressed also that the SW transformation is only applicable to the case of weak coupling between the localized electron state (5) and the conduction electrons as compared to the energy difference between the ground (singly occupied) and excited (empty and doubly occupied) localized states. As a consequence, the Hamiltonian (9) accurately describes the asymmetric Kondo problem under consideration for  $\Gamma_0 \ll [\varepsilon_F - \varepsilon_0, \varepsilon_0 - \varepsilon_F + U_C]$  and, therefore, the detunings  $D_{e,h}$  are assumed to meet the condition  $\Gamma_0 \ll D_{e,h}$ . Beyond the condition, the system enters the so-called mixed-valence regime, where the localized states (5) with different occupancy

become effectively coupled<sup>44</sup>. Although the mixed valence regime hosts a rich class of the interesting phase transitions, in the following we will focus exclusively at the Kondo regime, where the singly-occupied ground localized state is well separated from the excited states.

### III. RESULTS AND DISCUSSION

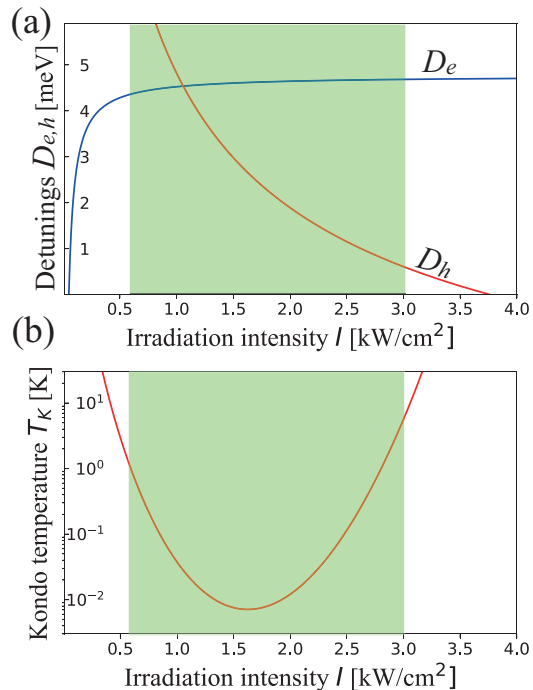


FIG. 2: Effect of the circularly polarized irradiation with the frequency  $\omega_0/2\pi = 200$  GHz and the intensity  $I$  on (a) the hole and electron detunings  $D_{h,e}$  and (b) the Kondo temperature in a GaAs-based QW filled by 2D electron gas with the Fermi energy  $\varepsilon_F = 5$  meV, energy broadening  $\Gamma_0 = 0.1\varepsilon_0$  and the electron effective mass  $m_e = 0.067m_0$  ( $m_0$  is the free electron mass) for the zero temperature. The green shadow areas mark the validity range of the model, where the applicability conditions are satisfied for both the Kondo Hamiltonian ( $\Gamma_0 \ll D_e, D_h$ ) and the dressed potential approach ( $\varepsilon_0 \ll \hbar\omega_0$ ).

For the particular case of 2D electrons in a GaAs-based QW, the dependence of the detunings  $D_{e,h}$  on the irradiation is plotted in Fig. 2a. It should be noted that excitations of virtual electrons and holes should be considered within the whole conduction band of width  $2D_0$ , where  $D_0 \approx 1.5$  eV for GaAs. Since the typical Kondo temperature is essentially smaller than the bandwidth  $D_0$ , one needs to transform the initial high-energy Hamiltonian (9) to the low-energy range in order to find the Kondo temperature. Such a transformation can be performed within the poor man's scaling renormalization approach<sup>45,47</sup>, which was originally proposed by Anderson. Following Anderson, the higher energy excitations corre-

sponding to the first order processes pictured in Fig. 3a can be integrated out from the Hamiltonian with using the SW transformation. Then the highest energy excitations, which are remained in the renormalized Hamiltonian, correspond to the second order processes pictured in Fig. 3b-c. It should be stressed that the renormalized Hamiltonian has the same structure as the initial one with the coupling constants depending on the renormalized (decreased) bandwidth  $D < D_0$ , where the renormalized coupling constant  $J(D)$  diverges at some critical bandwidth  $D = D_K$ . This critical bandwidth defines the sought Kondo temperature,  $T_K = D_K$ , which, particularly, indicates the applicability limit of the perturbation theory<sup>45,47</sup>.

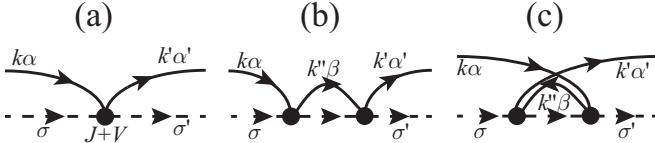


FIG. 3: The diagrams illustrating all possible first order processes (a) and the second order processes for electrons (b) and holes (c). The solid lines depict propagators of conduction electrons and holes, the dashed lines depict the localized spin propagator, whereas the symbols  $\sigma$  and  $\alpha(\beta)$  mark the spins of localized electrons and conduction electrons, respectively.

The only difference of the considered system from the original Kondo problem<sup>42</sup> is the strong electron-hole asymmetry since the typical Fermi energy in GaAs-based QWs is  $\varepsilon_F \ll D_0$ . As a consequence, the hole process shown in Fig. 3c cannot exist for  $D > \varepsilon_F$  and only the second order process involving a virtual electron (see Fig. 3b) should be taken into account. On the contrary, the both processes contribute to the effective coupling rescaling for the case of  $D < \varepsilon_F$ . Applying the known general solution of the asymmetric electron-hole Kondo problem<sup>46</sup> to the considered system, the flow equations for the effective exchange constant  $J'(D)$  and the scalar potential  $V'(D)$  can be written as

$$\begin{aligned} \frac{1}{\pi N_\varepsilon} \frac{\partial J'}{\partial \ln(D_0/D)} &= [1 + \theta(\varepsilon_F - D)]J'^2 - \theta(D - \varepsilon_F)J'V', \\ \frac{2}{\pi N_\varepsilon} \frac{\partial V'}{\partial \ln(D_0/D)} &= -\theta(D - \varepsilon_F) [3J'^2 + V'^2], \end{aligned} \quad (12)$$

with the boundary conditions  $J', V'|_{D=D_0} = J, V$ . The solving of Eqs. (12) should be performed in the two steps as follows. At the first step, we consider the interval  $\varepsilon_F \leq D \leq D_0$ . Within this interval, the two nonlinear differential equations (12) can be solved analytically (see, e.g., Ref. 46 for details) and result in the boundary condition

$$\begin{aligned} J'(\varepsilon_F) &= \\ &= \frac{J}{\left[1 + \frac{\pi N_\varepsilon}{2} \ln \frac{D_0}{\varepsilon_F} (J + V)\right] \left[1 - \frac{\pi N_\varepsilon}{2} \ln \frac{D_0}{\varepsilon_F} (3J - V)\right]}. \end{aligned} \quad (13)$$

At the second step, we consider the interval  $D \leq \varepsilon_F$ . Within this interval, the scalar potential  $V'$  is constant and the differential equation defining the effective exchange constant  $J'$  does not depend on the scalar potential. Therefore, the system of two nonlinear differential equations (12) is reduced to the two independent differential equations. Solving them under the boundary condition (13), one can find the effective exchange coupling constant  $J'(D)$ . Taking into account that the coupling constant diverges at the critical (Kondo) bandwidth  $D = D_K$ , we arrive the Kondo temperature

$$T_K = \varepsilon_F \exp \left[ -\frac{1}{2\pi N_\varepsilon J'(\varepsilon_F)} \right]. \quad (14)$$

Certainly, Eq. (14) turns into the known expression for the Kondo temperature  $T_K = D_0 \exp[-1/2J\pi N_\varepsilon]$  corresponding to the symmetric Kondo problem<sup>45</sup> if  $\varepsilon_F = D_0$  (the particular case of the half-filled band). The dependence of the Kondo temperature on the irradiation is plotted in Fig. 2b, where the Kondo temperature is found to be of several Kelvin. In the theory developed above, the field frequency,  $\omega_0$ , was assumed to satisfy the high-frequency condition  $\omega_0\tau \gg 1$ , where  $\tau$  is the mean free time of conduction electrons in the QW. To satisfy this condition for modern QWs and keep the irradiation intensity  $I$  to be reasonable, we chose the field frequency for our calculations (see Fig. 2) near the upper limit of microwave range,  $\omega_0/2\pi = 200$  GHz, which can be easily realized in experiments. It should be noted also that the present theory is developed for the case of symmetric QW, although effects in asymmetric QWs are also studied actively (see, e.g., Refs. 48,49). In such asymmetric QWs, particularly, there is the Rashba spin-orbit coupling which can lead to the exponential increase of the Kondo temperature<sup>50</sup>.

To observe the discussed effect experimentally, the known contribution of the Kondo resonance to the electron mean free time<sup>1</sup>,

$$1/\tau \sim J^4 \left[ \frac{1}{\pi N_\varepsilon J} + 2 \ln \frac{D_0}{T} \right]^2, \quad (15)$$

can be used. Indeed, the found Kondo temperature (14) corresponds to the minimum of the contribution (15) as a function of the temperature  $T$ . Since all electron transport phenomena depend on the electron mean free time  $\tau$ , this minimum can be detected in various transport experiments (e.g., conductivity measurements). In order to exclude effects arisen from the irradiation-induced heating of electron gas, the difference scheme based on using both a circularly polarized field and a linearly polarized one can be applied. Indeed, the heating does not depend on the field polarization, whereas the electron states bound at repulsive scatterers — and the related Kondo effect, respectively — can be induced only by a circularly polarized field<sup>39</sup>.

#### IV. CONCLUSION

We showed within the Floquet theory that a circularly polarized electromagnetic field irradiating a two-dimensional electron system can induce the localized electron states which antiferromagnetically interact with conduction electrons. As a consequence, the Kondo effect appears. For semiconductor quantum wells irradiated by a microwave electromagnetic wave of the inten-

sity  $\sim \text{kW/cm}^2$ , the Kondo temperature is found to be of several Kelvin and, therefore, the effect can be detected in state-of-the-art transport measurements.

#### V. ACKNOWLEDGEMENTS

The reported study was funded by the Russian Science Foundation (project 20-12-00001).

- 
- \* Electronic address: Oleg.Kibis(c)nstu.ru
- <sup>1</sup> Kondo G Resistance 1964 Minimum in Dilute Magnetic Alloys *Progress of Theoretical Physics* **32** 37
  - <sup>2</sup> De Haas W J, De Boer J and Van den Berg G J 1934 The electrical resistance of gold, copper and lead at low temperatures *Physica* **1** 1115
  - <sup>3</sup> Wilson K G 1973 The renormalization group: Critical phenomena and the Kondo problem *Rev. Mod. Phys.* **47** 773
  - <sup>4</sup> Fateev V A and Wiegmann P B 1981 The exact solution of the s-d exchange model with arbitrary impurity spin S (Kondo problem) *Phys. Lett. A* **81** 179
  - <sup>5</sup> Andrei N, Furuya K and Lowenstein J H 1983 Solution of the Kondo problem *Rev. Mod. Phys.* **55** 331
  - <sup>6</sup> Steglich F, Aarts J, Bredl C D, Lieke W, Meschede D, Franz W and Schäfer H 1979 Superconductivity in the Presence of Strong Pauli Paramagnetism: CeCu<sub>2</sub>Si<sub>2</sub> *Phys. Rev. Lett.* **43** 1892
  - <sup>7</sup> Andres K, Graebner J E and Ott H R 1975 4f-Virtual-Bound-State Formation in CeAl<sub>3</sub> at Low Temperatures *Phys. Rev. Lett.* **35** 1779
  - <sup>8</sup> Tsunetsugu H, Sigrist M and Ueda K 1993 Phase diagram of the one-dimensional Kondo-lattice model *Phys. Rev. B* **47** 8345
  - <sup>9</sup> Stewart G R 1984 Heavy-fermion systems *Rev. Mod. Phys.* **56** 755
  - <sup>10</sup> Kouwenhoven L and Glazman L 2001 Revival of the Kondo effect *Phys. World* **14**(1) 33
  - <sup>11</sup> Goldhaber-Gordon D, Göres J, Kastner M A, Shtrikman H, Mahalu D and Meirav U 1998 From the Kondo Regime to the Mixed-Valence Regime in a Single-Electron Transistor *Phys. Rev. Lett.* **81** 5225
  - <sup>12</sup> Cronenwett S M, Oosterkamp T H and Kouwenhoven L P 1998 A Tunable Kondo Effect in Quantum Dots *Science* **281** 540
  - <sup>13</sup> Iftikhar Z, Anthore A, Mitchell A, Parmentier F, Gennser U, Querghi A, Cavanna A, Mora C, Simon P and Pierre F 2018 Tunable quantum criticality and super-ballistic transport in a “charge” Kondo circuit *Science* **360** 1315
  - <sup>14</sup> Park J, Pasupathy A N, Goldsmith J I, Chang C, Yaish Y, Petta J R, Rinkoski M, Sethna J P, Abruna H D, McEuen P L and Ralph D C 2002 Coulomb blockade and the Kondo effect in single-atom transistors *Nature* **417** 722
  - <sup>15</sup> Borzenets I V, Shim J, Chen J C H, Ludwig A, Wieck A D, Tarucha S, Sim H-S and Yamamoto M 2020 Observation of the Kondo screening cloud *Nature* **579** 210
  - <sup>16</sup> Latta C, Haupt F, Hanl M, Weichselbaum A, Claassen M, Wuester W, Fallahi P, Faelt S, Glazman L, von Delft J, Türeci H E and Imamoglu A 2011 Quantum quench of Kondo correlations in optical absorption *Nature* **474** 627
  - <sup>17</sup> Haupt F, Smolka S, Hanl M, Wüster W, Miguel-Sanchez J, Weichselbaum A, von Delft J and Imamoglu A 2013 Nonequilibrium dynamics in an optical transition from a neutral quantum dot to a correlated many-body state *Phys. Rev. B* **88** 161304
  - <sup>18</sup> Türeci H E, Hanl M, Claassen M, Weichselbaum A, Hecht T, Braunecker B, Govorov A, Glazman L, Imamoglu A and von Delft J 2011 Many-Body Dynamics of Exciton Creation in a Quantum Dot by Optical Absorption: A Quantum Quench towards Kondo Correlations *Phys. Rev. Lett.* **106** 107402
  - <sup>19</sup> Sbierski B, Hanl M, Weichselbaum A, Türeci H E, Goldstein M, Glazman L I, von Delft J and Imamoglu A 2013 Proposed Rabi-Kondo Correlated State in a Laser-Driven Semiconductor Quantum Dot *Phys. Rev. Lett.* **111** 157402
  - <sup>20</sup> Nakagawa M and Kawakami N 2015 Laser-Induced Kondo Effect in Ultracold Alkaline-Earth Fermions *Phys. Rev. Lett.* **115** 165303
  - <sup>21</sup> Basov D N, Averitt R D and Hsieh D 2017 Towards properties on demand in quantum materials *Nat. Mater.* **16** 1077
  - <sup>22</sup> Oka T and Kitamura S 2019 Floquet Engineering of Quantum Materials *Ann. Rev. Cond. Matt. Phys.* **10** 387
  - <sup>23</sup> Goldman N and Dalibard J 2014 Periodically Driven Quantum Systems: Effective Hamiltonians and Engineered Gauge Fields *Phys. Rev. X* **4** 031027
  - <sup>24</sup> Bukov M, D’Alessio L and Polkovnikov A 2015 Universal high-frequency behavior of periodically driven systems: From dynamical stabilization to Floquet engineering *Adv. Phys.* **64** 139
  - <sup>25</sup> Lindner N H, Refael G and Galitski V 2011 Floquet topological insulator in semiconductor quantum wells *Nat. Phys.* **7** 490
  - <sup>26</sup> Savenko I G, Kibis O V and Shelykh I A 2012 Asymmetric quantum dot in a microcavity as a nonlinear optical element *Phys. Rev. A* **85** 053818
  - <sup>27</sup> Rechtsman M C, Zeuner J M, Plotnik Y, Lumer Y, Podolsky D, Dreisow F, Nolte S, Segev M and Szameit A 2013 Photonic Floquet topological insulator *Nature* **496** 196
  - <sup>28</sup> Wang Y H, Steinberg H, Jarillo-Herrero P and Gedik N 2013 Observation of Floquet-Bloch states on the surface of a topological insulator *Science* **342** 453
  - <sup>29</sup> Glazov M M and Ganichev S D 2014 High frequency electric field induced nonlinear effects in graphene *Phys. Rep.* **535** 101
  - <sup>30</sup> Usaj G, Perez-Piskunow P M, Foa Torres L E F and Balseriro C A 2014 Irradiated graphene as a tunable Floquet topological insulator *Phys. Rev. B* **90** 115423
  - <sup>31</sup> Sentef M A, Claassen M, Kemper A F, Moritz B, Oka T,

- Freericks J K and Devereaux T P 2015 Theory of Floquet band formation and local pseudospin textures in pump-probe photoemission of graphene *Nat. Commun.* **6** 7047
- <sup>32</sup> Sie E J, McIver J W, Lee Y-H, Fu L, Kong J and Gedik N 2015 Valley-selective optical Stark effect in monolayer WS<sub>2</sub> *Nat. Mater.* **14** 290
- <sup>33</sup> Dini K, Kibis O V and Shelykh I A 2016 Magnetic properties of a two-dimensional electron gas strongly coupled to light *Phys. Rev. B* **93** 235411
- <sup>34</sup> Kibis O V, Dini K, Iorsh I V and Shelykh I A 2017 All-optical band engineering of gapped Dirac materials *Phys. Rev. B* **95** 125401
- <sup>35</sup> Iorsh I V, Dini K, Kibis O V and Shelykh I A 2017 Optically induced Lifshitz transition in bilayer graphene *Phys. Rev. B* **96** 155432
- <sup>36</sup> Kozin V K, Iorsh I V, Kibis O V and Shelykh I A 2018 Quantum ring with the Rashba spin-orbit interaction in the regime of strong light-matter coupling *Phys. Rev. B* **97** 155434
- <sup>37</sup> Kozin V K, Iorsh I V, Kibis O V and Shelykh I A 2018 Periodic array of quantum rings strongly coupled to circularly polarized light as a topological insulator *Phys. Rev. B* **97** 035416
- <sup>38</sup> McIver J W, Schulte B, Stein F-U, Matsuyama T, Jotzu G, Meier G and Cavalleri A 2020 Light-induced anomalous Hall effect in graphene *Nat. Phys.* **16** 38
- <sup>39</sup> Kibis O V 2019 Electron pairing in nanostructures driven by an oscillating field *Phys. Rev. B* **99** 235416
- <sup>40</sup> Kibis O V, Boev M V and Kovalev V M 2020 Light-induced bound electron states in two-dimensional systems: Contribution to electron transport *Phys. Rev. B* **102** 075412
- <sup>41</sup> Kibis O V, Kolodny S A and Iorsh I V 2021 Fano resonances in optical spectra of semiconductor quantum wells dressed by circularly polarized light *Opt. Lett.* **46** 50
- <sup>42</sup> Anderson P W 1961 Localized Magnetic States in Metals *Phys. Rev.* **124** 41
- <sup>43</sup> Coleman P 2015 *Introduction to many-body physics* (Cambridge: University Press)
- <sup>44</sup> Riseborough P S and Lawrence J M 2016 Mixed Valent Metals *Rep. Prog. Phys.* **79** 084501
- <sup>45</sup> Anderson P W 1979 A poor man's derivation of scaling laws for the Kondo problem *J. Phys. C: Solid State Phys.* **3** 2436
- <sup>46</sup> Zitko R and Hovrat A 1994 Kondo effect at low electron density and high particle-hole asymmetry in 1D, 2D, and 3D *Phys. Rev. B* **94** 125138
- <sup>47</sup> Anderson P W Kondo effect 1973 *Comments on Solid State Phys.* **5** 73
- <sup>48</sup> Stavrou V N, Babiker M and Bennett C R 2001 Influences of asymmetric quantum wells on electron-phonon interactions *J. Phys.: Condens. Matter* **13** 6489
- <sup>49</sup> Arulmozhi R, John Peterb A and Lee C W 2020 Optical absorption in a CdS/CdSe/CdS asymmetric quantum well *Chem. Phys. Lett.* **742** 137129
- <sup>50</sup> Wong A, Ulloa S E, Sandler N and Ingersent K 2016 Influence of Rashba spin-orbit coupling on the Kondo effect *Phys. Rev. B* **93** 075148